SUPPLEMENTAL MATERIAL

Metabolic Trajectories Following Contrasting Prudent and Western Diets from Food Provisions: Robust Biomarkers of Short-term Changes in Habitual Diet

Nadine Wellington,[1] Meera Shanmuganathan,[1] Russell J. de Souza,[2,3] Michael Zulyniak,[2] Sandi Azab,[1] Jonathon Bloomfield,[1] Alicia Mell,[1] Ritchie Ly,[1] Dipika Desai,[2] Sonia S. Anand,[2,3] and Philip Britz-McKibbin[1]

[1] *Department of Chemical and Chemical Biology, McMaster University, Hamilton, ON, Canada*

[2] *Department of Medicine, McMaster University, Hamilton, ON, Canada*

[3] *Department of Clinical Epidemiology and Biostatistics, McMaster University, Hamilton, ON Canada*

***** Corresponding author: Philip Britz-McKibbin, britz@mcmaster.ca

Experimental, Tables S1-S2; Figures S1-S14

1. EXPERIMENTAL

1.1 Chemicals and Reagents. Ultra HPLC grade LC-MS solvents (water, methanol, acetonitrile) obtained from Caledon Laboratories Ltd. (Georgetown, ON, Canada) were used to prepare all buffer and sheath liquid solutions, unless otherwise stated. Proline betaine was purchased from Toronto Research Chemicals (Toronto, Ontario, Canada). All other chemicals were obtained from Sigma-Aldrich Inc. (St. Louis, MO, USA).

1.2 Nontargeted Metabolite Profiling of Plasma and Urine by MSI-CE-MS. Fasting plasma (EDTA) samples together with matching single-spot urine samples were collected from all DIGEST participants during clinic visits on day 1 and day 14, which were then stored at -80 °C [1]. Multisegment injection-capillary electrophoresis-mass spectrometry (MSI-CE-MS) was the major platform used for nontargeted profiling of polar/ionic metabolites from both plasma and urine samples [2], which was performed on an Agilent G7100A CE (Agilent Technologies Inc., Mississauga, ON, Canada) equipped with a coaxial sheath liquid (Dual AJS) Jetstream electrospray ion source coupled to an Agilent 6230 TOF-MS system. All separations were performed using uncoated fused-silica capillaries (Polymicro Technologies, AZ, USA) with a total length of 120 cm and inner diameter of 50 μm. About 7 mm of polyimide coating was removed from both distal ends to avoid sample carry-over and prevent polyimide swelling when it contacts with organic solvent [3]. The background electrolyte (BGE) consisted of 1 M formic acid with 15% *vol* acetonitrile (pH 1.80) under positive ion mode, and 50 mM ammonium bicarbonate (pH 8.50) under negative ion mode for analysis of the ionic metabolome, including cationic and anionic metabolites from matching plasma and urine specimens, respectively. All CE separations were performed under normal polarity with an applied voltage of 30 kV at 25 °C. However, a pressure gradient of 2 mbar/min from 0 to 40 min was used for MSI-CE-MS analyses under negative ion mode conditions to shorten analysis times for highly charged anionic metabolites (*e.g.,* citrate). The TOF-MS system was operated with full-scan data acquisition over a mass range of *m/z* 50-1700 and an acquisition rate of 500 ms/spectrum. The sheath liquid was comprised of 60% *vol* MeOH with 0.1% vol formic acid for positive ion mode, and 50% *vol* MeOH for negative ion mode. The ESI conditions were Vcap =2000 V, nozzle voltage = 2000 V, nebulizer gas =10 psi, sheath gas = 3.5 L/min at 195 °C, drying gas 8 L/min at 300 °C. whereas, the MS voltage settings were fragmentor = 120 V, skimmer = 65V and Oct1 RF= 750 V.

A seven sample serial injection format was used in MSI-CE-MS [2-6] consisting of a serial injections of six discrete samples together with a pooled quality control (QC) within each experimental run; the latter sample was used to assess technical variance while also allowing for robust batch correction due to long-term signal drift in ESI-MS [5,7]. Multiplexed separations in MSI-CE-MS was performed by programming a hydrodynamic injection sequence with each sample (5 s at 100 mbar) interspaced with a BGE spacer (40 s at 100 mbar) prior to voltage application as described elsewhere [2-6]. In this study, nontargeted metabolite profiling of plasma or urine specimens by MSI-CE-MS was performed by pairing together matching baseline and post-treatment samples for three individual DIGEST participants together with a QC in a randomized injection position for each run. Different serial sample injection configurations in MSI-CE-MS were also applied for rigorous metabolite authentication using a dilution trend filter, as well as acquisition of calibration curves for reliable quantification of metabolites. Briefly, authentic metabolites were defined by their unique accurate mass and relative migration time (*m/z*:RMT) under positive (+) or negative (-) ion mode detection after filtering out spurious signals, background ions, as well as redundant adducts/in-source fragments and isotopic features that comprise the majority of signals when performing MS-based metabolomics [8]. Additionally, only frequently detected plasma or urinary metabolites measured in the majority of samples from DIGEST participants (> 75%) with acceptable technical precision based on repeated analysis of QCs (mean CV < 30%) were included in the final metabolomics data matrix (Table S1) as a way to reduce false discoveries and data overfitting. Missing (*i.e.,* zero) data below method detection limits were replaced with a minimum value corresponding to half of the lowest response measured for a given metabolite in all samples analyzed.

1.3 Unknown Metabolite Identification by MS/MS. In all cases, authenticated metabolites defined by their *m/z*:RMT under positive (+) or negative (-) ion mode detection were further characterized by their most likely molecular formula, mass error (< 10 ppm) and overall technical precision (%CV) from pooled plasma or urine samples. High resolution tandem mass spectrometry (MS/MS) was employed for structural elucidation of unknown metabolites of biological significance from pooled samples in this study. Targeted MS/MS experiments were performed on an Agilent G7100A CE system with a coaxial sheath liquid Jetstream electrospray ion source connected to an Agilent 6500 iFunnel QTOF instrument. Metabolite identification in

this work adopted reporting standards recommended from the Metabolomics Standards Initiative [9], including unambiguous identification (level 1) that is confirmed with matching MS/MS spectra and co-migration by authentic standard acquired on the same instrument, tentative/probable identification (level 2) by comparison of MS/MS spectra from public databases or published literature, partial annotation of MS/MS spectra guided by *in silico* software tools with metabolite class (level 3), and compounds with unknown chemical structure (level 4). The latter case typically occurred for low abundance metabolites that had inadequate responses for their precursor ion when acquiring MS/MS spectra via collision-induced dissociation (CID) experiments. In our case, the electromigration behavior of polar/ionic metabolites (*i.e.,* electrophoretic mobility or RMT) provided additional information that complemented MS/MS when selecting among potential isobaric or isomeric candidate ions, in addition to their likely biochemical relevance in human plasma or urine. MS/MS spectra were acquired from pooled plasma or urine samples that were injected hydrodynamically using a conventional single sample injection plug at 50 mbar for 10 s followed by 5 s with BGE. Precursor ions were selected for CID experiments at 10, 20 and 40 V. Mirror plots comparing MS/MS spectra of unknown metabolites under an optimal collision energy were then compared to their respective authentic reference standard if available, which were generating using the "InterpretMSSpectrum" R Package. Otherwise, MS/MS spectra were annotated based on their characteristic product ions or neutral losses for *de novo* structural elucidation (level 2 or 3), which was guided by *in silico* MS/MS spectra generated by CFM-ID [10] or comparison to MS/MS spectra deposited in open-access public repositories (HMDB, http://www.hmdb.ca) or published in literature (if available). The exact stereochemistry of certain metabolites identified in plasma or urine were uncertain if authentic standards were not available for confirmation.

1.4 Total Plasma Fatty Acid Determination by GC-MS. A GC-MS method was used for targeted analysis of total (hydrolyzed) fatty acids (FA) and their isomers from plasma extracts on an Agilent 6890 GC coupled to an Agilent 5973 single quadrupole mass spectrometer with electron impact ionization (EI) as described elsewhere with minor modifications [11]. Total hydrolyzed plasma FA were analyzed by GC-MS as their methyl ester derivatives (FAME) using *N*-methyl-*N*-(trimethylsilyl)trifluoroacetamide (MSTFA) (≥ 98.5%, GC from Sigma-Aldrich). Isotopically-labelled myristic acid-d27 (98%), stearic acid-d35 (98%) and pyrene-d10 (98%) were obtained

from Cambridge Isotope Laboratories (Tewksbury, MA, USA). HPLC grade chloroform (≥ 99.5%, GC), methanol (99.8%, GC), hexanes (≥ 99.5%, GC) and Ultra LC-MS grade water were purchased from Caledon Laboratories Ltd. (Georgetown, ON, Canada). The antioxidant, butylated hydroxytoluene (BHT, 490 µL) was added to all fatty acids calibrant solutions prepared in methanol to prevent autooxidation. Briefly, a 10 µL aliquot of thawed plasma was mixed with 5 µL of a 1.0 mg/mL C18:0-d35 recovery standard. Concentrated sulfuric acid (10 µL) was added as a transesterification catalyst and vortexed for 2 min before incubation for 4 h at 80 ºC to produce FAMEs for improved volatility. Cooled samples were then mixed with 500 µL of 9 g/L NaCl and 200 µL hexanes and vortexed for 2 min prior to centrifugation at 14,000 *g* at 4 ºC for 5 min. GC inserts were prepared with 45 µL of hexane supernatant with 5 µL of internal standard pyrene-d10 and vortexed for 2 min before injection. Total plasma FAMEs were resolved on a Supleco SP-2380 column (30 m x 0.25 mm x 0.20 µM) using an optimal temperature program within 30 min.[6] Samples were injected in 1.0 µL volumes using a splitless injector held at 250 °C, the carrier gas was helium at 1.0 mL/min and the transfer line was held at 270 °C. Relative abundances were measured on the relative response of a quantifying ion (*e.g.,* $[M\text{-}15]^+$) relative to the pyrene-d10 internal standard. Pooled plasma samples as QC and blank extracts were analyzed together with each batch of 8-10 randomized plasma samples from DIGEST participants when using GC-MS in order to assess technical precision and monitor for background contamination. A temperature program used for resolution of major trimethylsiylated fatty acids from plasma hydrolysates comprised of a temperature gradient of 20 °C/min starting from 2 min at 80 °C until 20 min at 160 °C, which was further increased to 190 °C for 3 min prior to elution at 300 °C for 5 min with a total run time of 28 min. In most cases, FAMEs were quantified in GC-MS based on integration of the relative response ratio of their [M-15]+ fragment ion relative to pyrene-d10 as internal standard when using single ion monitoring (SIM) mode detection. Calibrations curves from a serial dilution of fatty acid standards were subsequently used for their quantification, as well as their identification when comparing their characteristic EI-MS spectra (70 eV) and elution times (*i.e.,* co-elution with spiking).

1.5 Targeted Urinary Electrolyte Analysis. Targeted analysis of inorganic/involatile electrolytes in urine was performed using two complementary CE-UV methods adapted from Nori de Macedo *et al.* [12] and Saoi *et al*. [5] for anionic (*e.g.,* nitrate) and cationic (*e.g.,* sodium) electrolytes, respectively. Analysis of major cationic electrolytes was performed on diluted urine samples that

were thawed, vortexed for 30 s and centrifuged at 14,000 *g* for 5 min. An aliquot of the supernatant was diluted with deionized water and spiked with 0.5 mM lithium as an internal standard. Samples were analyzed on an Agilent G7100A CE system with UV photodiode array detection with indirect absorbance detection at 214 nm. All samples were injected hydrodynamically for 10 s (at 35 mbar) and separation was performed under normal polarity at 30 kV at 25°C using a 50 µm inner diameter capillary with 60 cm total length. The background electrolyte (BGE) was 5 mM formic acid containing 12.5 mM creatinine (Crn) and 4 mM 18-crown-6 ether at pH 4.0 (adjusted with 1 M sulfuric acid. In this case, ammonium (NH_4^+), sodium (Na^+), potassium (K^+), calcium (Ca^{2+}) and magnesium (Mg^{2+}) were analyzed in urine samples.[5] Additionally, all urine samples were analyzed using a complementary CE assay for UV-absorbing inorganic anions, including nitrate (NO_3^-), iodide (I^-) and thiocyanate (SCN^-) as described elsewhere [12]. In this case, the BGE was comprised of 180 mM lithium hydroxide, 180 mM phosphoric acid, and 10 mM α-cyclodextrin (α-CD) at pH 3.0 (adjusted with 1 M phosphoric acid), where 1,5-naphthalene disulfonate (NDS) was used as an internal standard. Samples were injected hydrodynamically for 80 s at 0.5 psi and analyzed at 25 °C under a reversed polarity at -18 kV with UV absorbance detection at 226 nm (288 nm for NDS). In both CE-UV assays, a pooled urine sample serving as a QC was measured intermittently after every batch of 6 random urine samples. In all cases, creatinine concentrations were measured by MSI-CE-MS under positive ion mode conditions, which were used to reduce biological variance and correct for differences in hydration status for single-spot urine samples analyzed in this study.

1.6 Data Preprocessing and Statistical Analysis. All MSI-CE-MS data were integrated and analyzed using Agilent MassHunter Qualitative Analysis B.07.00 and Microsoft Excel and Igor (Wavemetrics Inc., OR, USA). In all cases, the integrated ion response (*i.e.,* peak area) for each metabolite was normalized to an internal standard, 4-chlorotyrosine (Cl-Tyr) migrating from the same sample by MSI-CE-MS. Also, a QC-based batch correction algorithm was applied to creatinine-normalized urine metabolomic data to adjust for long-term signal drift in ESI-MS during data acquisition as outlined in a recent work [5]. This algorithm is based on an empirical Bayesian frameworks [7] that takes advantage of the QC samples included in each serial injection run when using MSI-CE-MS, as well as batch and injection sequence information. However, batch correction did not provide any significant improvement in the overall technical precision of

plasma metabolome data and thus was not necessary to perform in this case. All non-batch (plasma) and batch-corrected (urine) metabolomic data was pre-processed using generalized *log*-transformation and autoscaling prior to multivariate statistical analysis using MetaboAnalyst 4.0 (www.metaboanalyst.ca) [13], including volcano plots, principle component analysis (PCA), hierarchical cluster analysis (HCA)/2D heat maps, receiver operating characteristic (ROC) curves, orthogonal partial least squares-discriminant analysis (OPLS-DA), as well as multivariate empirical Bayes analysis (MEBA) of variance; the latter method is optimal when analyzing time-series data [14] as related to metabolic trajectories. To validate each OPLS-DA model, cross-validation and permutation testing (n = 1000) on paired metabolome data sets (*i.e.,* ratio of metabolite response based on assigned diet/baseline diet for each subject) following *glog* transformation and autoscaling, whereas Hotelling's *T*-squared distribution using MEBA was performed on *glog*-transformed metabolomic time series data from DIGEST participants at baseline and following two weeks of assigned food provisions. These complementary statistical approaches were initially used for unsupervised data exploration to identify overall trends, as well as supervised data analysis for ranking metabolite candidates modulated by contrasting assigned diets among DIGEST participants without adjustments for covariates. Additionally, normality tests, partial Pearson correlation analysis, and mixed model ANOVA were performed on top-ranked dietary biomarker candidates using the Statistical Package for the Social Sciences (SPSS, version 18.0). In this case, a partial listwise Pearson correlation analysis of lead plasma and creatinine-normalized metabolite responses to 20 major nutrient categories from self-reported food records from DIGEST participants (n=42) were adjusted for age, sex, and post-intervention BMI. Only metabolites that had a correlation coefficient of $r > \pm 0.300$ and $p < 0.05$ for more than two nutrient categories were considered significant in this work. A repeat measures general linear mixed ANOVA model was also performed with the number of levels set at 2 for the repeat sampling (*i.e.,* time; baseline habitual diet and assigned diet after 2 weeks) while setting the intervention diet (*i.e.,* treatment arm; P-W or W-P) as the between-subject factor with age, sex and post-intervention *BMI* as potential covariates. Overall, plasma and urine metabolites reflecting contrasting dietary patterns assigned to DIGEST participants that satisfied MEBA and/or mixed ANOVA, as well as partial correlation analysis to two or more nutrient categories from self-reported diet records were considered as robust dietary biomarkers.

2. Supporting References

76. Zulyniak, M. A.; de Souza, R. J.; Mente, A.; Kandasamy, S.; Nundy, M.; Desai, D.; Raman, K.; Hasso, R.; Paré, G.; Beyene, J., Anand, S. S. A randomized controlled trial of the effects of a Prudent diet on cardiovascular risk factors, gene expression, and DNA methylation - the Diet and Genetic Intervention (DIGEST) pilot study. *BMC Nutr.* **2016**, *2*, 34.
77. Kuehnbaum, N. L.; Kormendi, A.; Britz-McKibbin, P. Multisegment injection-capillary electrophoresis-mass spectrometry: A high-throughput platform for metabolomics with high data fidelity. *Anal. Chem.* **2013**, *85*, 10664-10669.
78. Yamamoto, M.; Ly, R.; Gill, B.; Zhu, Y.; Moran-Mirabal, J.; Britz-McKibbin, P. Robust and high-throughput method for anionic metabolite profiling: Preventing polyimide aminolysis and capillary breakages under alkaline conditions in capillary electrophoresis-mass spectrometry. *Anal. Chem.* **2016**, *88*, 10710–10719.
79. Nori de Macedo, A.; Mathiaparanam, S.; Brick, L.; Keenan, K.; Gonska, T.; Pedder, L.; Hill, S.; Britz-McKibbin, P. The sweat metabolome of screen-positive cystic fibrosis infants: Revealing mechanisms beyond impaired chloride transport. *ACS Cent. Sci.* **2017**, *3*, 904–913.
80. DiBattista, A.; McIntosh, N.; Lamoureux, M.; Al-Dirbashi, O. Y.; Chakraborty, P.; Britz-McKibbin, P. Metabolic signatures of cystic fibrosis identified in dried blood spots for newborn screening without carrier identification. *J. Proteome Res.* **2019**, *18*, 841–854.
81. Saoi, M.; Percival, M.; Nemr, C.; Li, A.; Gibala, M. J.; Britz-McKibbin, P. Characterization of the human skeletal muscle metabolome for elucidating the mechanisms of bicarbonate ingestion on strenuous interval exercise. *Anal. Chem.* **2019**, *91*, 4709–4718.
82. Wehrens, R.; Hageman, J. A.; van Eeuwijk, F.; Kooke, R.; Flood, P. J.; Wijnker, E.; Keurentjes, J. J. B.; Lommen, A.; van Eekelen, H. D. L. M.; Hall, R. D.; Mumm, R.; de Vos, R. C. H. Improved batch correction in untargeted MS-based metabolomics. *Metabolomics* **2016**, *12*, 88.
83. Mahieu, N. G.; Patti, G. J. Systems-level annotation of a metabolomics data set reduces 25 000 features to fewer than 1000 unique metabolites. *Anal. Chem.* **2017**, *89*, 10397–10406.
84. Dunn, W. B., Erban, A., Weber, R. J. M., Creek, D. J., Brown, M., Breitling, R., Hankemeier, T.; Goodacre, R.; Neumann, S.; Kopka, J.; Viant, M. R. Mass appeal: Metabolite identification in mass spectrometry-focused untargeted metabolomics. *Metabolomics* **2013**, *9*, 44–66.
85. Allen, F.; Pon, A.; Wilson, M.; Greiner, R.; Wishart, W. CFM-ID: A web server for annotation, spectrum prediction and metabolite identification from tandem mass spectra. *Nucleic Acids Res.* **2014**, *42*, W94–W99.
86. Jafari, N.; Ahmed, R.; Gloyd, M.; Bloomfield, J.; Britz-McKibbin, P.; Melacini G. Allosteric sensing of fatty acid binding by NMR: Application to human serum albumin. *J. Med. Chem.* **2016**, *59*, 7457-7465.
87. Nori de Macedo, A. N.; Teo, K.; Mente, A.; McQueen, M. J.; Zeidler, J.; Poirier, P.; Lear, S. A.; Wielgosz, A.; Britz-McKibbin, P. A robust method for iodine status determination in epidemiological studies by capillary electrophoresis. *Anal. Chem.* **2014**, *86*, 10010–10015.
88. Chong, J.; Soufan, O.; Li, C.; Caraus, I.; Li, S.; Bourque, G.; Wishart, D. S.; Xia, J. MetaboAnalyst 4.0: towards more transparent and integrative metabolomics analysis. *Nucleic Acids Res.* **2018**, *46*,W486-W494.
89. Tai, B. Y.; Speed, T. P. A multivariate empirical Bayes statistic for replicated microarray time course data. *Ann. Statistics* **2006**, *34*, 2387–2412.

Table S1. Baseline group characteristics of a cohort of healthy participants (*n*=42) recruited in a two-arm parallel randomized clinical trial to compare the effects of a contrasting diet over 2 weeks (Western or Prudent) from food provisions reflecting changes in habitual dietary patterns.

Variable	Prudent assigned W-P, *n*=24	Western assigned P-W, *n*=18	Significance/comments[b]
Sex (n; %)	--	--	$p > 0.05$; More females than
F	66%, n=16	61%, n= 11	males recruited in each arm
M	33%, n= 8	39%, n = 7	
Age (mean)	(50 ± 18)	(43 ± 20)	$p > 0.05$; Wide disparity in age
< 50 y	(29 ± 9 n=9)	(28 ± 10, n=10)	with no differences between
> 50 y	(62 ± 7, n=15)	(63 ± 8, n=8)	arms
BMI (mean)	(28 ± 6)	(26 ± 6)	$p > 0.05$; Wide disparity in body
Lean (19-24.9 kg/m^2)	(23 ± 2, n=7)	(22 ± 2, n=11)	composition and no differences
Overweight/obese (25-44 kg/m^2)	(30 ± 5, n=17)	(31 ± 5, n=7)	between arms
Habitual baseline diet index[a]	--	--	$p = 0.0037$; Greater western
Prudent diet score (< 0.5)	(0.42 ± 0.93)	(0.92 ± 0.68)	habitual dietary patterns in
Western diet score (> 1.0)	(3.4 ± 0.9)	(0.70 ± 1.31)	prudent assigned arm
Average caloric intake (kcal)	(1985 ± 560)	(1895 ± 640)	$p > 0.05$
Average fiber intake (/2000 kcal)	(21.3 ± 6.3); 24	(26.6 ± 8.5); 18	$p = 0.018$; Higher intake of fiber in western assigned arm
Average poly:sat fatty acid (ratio)	(0.44 ± 0.16); 24	(0.58 ± 0.16); 18	$p = 0.0067$; Higher poly:sat intake in western assigned arm
Average energy from sat. fat (%)	(11.9 ± 3.2); 24	(9.8 ± 2.0); 18	$p = 0.015$; Higher sat. fat intake in prudent assigned arm
Urinary Na/K (ratio)	(1.31 ± 0.72); 24	(0.80 ± 0.55); 18	$p = 0.016$; Higher Na/K intake in prudent assigned arm
Fasting glucose (mM)	(5.1 ± 1.0)	(4.9 ± 0.4)	$p > 0.05$
LDL cholesterol (mM)	(3.1 ± 1.0)	(2.8 ± 0.9)	$p > 0.05$
HDL cholesterol (mM)	(1.55 ± 0.42)	(1.46 ± 0.44)	$p > 0.05$
Total cholesterol (mM)	(5.2 ± 1.3)	(5.0 ± 1.0)	$p > 0.05$
Triglycerides (mM)	(0.63 ± 0.18)	(0.61 ± 0.18)	$p > 0.05$
ApoB/ApoA1 ratio	(1.24 ± 0.77)	(1.0 ± 0.18)	$p > 0.05$
CRP (mg/L)	(2.4 ± 4.1)	(2.2 ± 2.9)	$p > 0.05$
IL-8 (ng/L)	(9.1 ± 6.5)	(6.8 ± 2.1)	$p > 0.05$
Average systolic BP (mmHg)	(121 ± 18)	(114 ± 17)	$p > 0.05$
Average dystolic BP (mmHg)	(78 ± 11)	(74 ± 10)	$p > 0.05$

[a] *Self-reported diet index score at baseline was used as a single aggregate index to categorize dietary patterns as predominately Prudent or Western in terms of average daily intake of total fiber, fruit & vegetables, potassium, polyunsaturated/saturated fatty acid ratio and % saturated fatty acids.*

[b] *There were no significant differences ($p < 0.05$) in classic serum/plasma biomarkers of CVD risk at baseline, as well as following 2-week dietary intervention between treatment arm among subjects in this study.*

Table S2. Summary of representative and reliably measured urinary and plasma metabolites detected inmajority of DIGEST participants patients that are annotated based on their accurate mass (*m/z*), relative migration time (RMT), ionization mode (*p* = ESI+, *n* = ESI-), most likely molecular formula, compound name, confidence level for identification, and technical precision from QC measurements.

Biofluid	*m/z:RMT:polarity*	*Molecular formula*[a]	*Monoisotopic mass*	*Δm (ppm)*	*Compound ID*	*HMDB ID*	*Level of Confidence*[b]	*%CV*[c]
Urine	76.0757 : 0.546:+	C_3H_9NO	76.0757	0.0	Trimethylamine *N*-oxide	HMDB00925	2	9.86
Urine	104.0706 : 0.667:+	$C_4H_9NO_2$	104.0706	0.0	γ-Aminobutyic acid	HMDB00112	2	39.69
Urine	104.0706 : 0.928:+	$C_4H_9NO_2$	104.0706	0.0	Dimethylglycine	HMDB0000092	2	33.80
Urine	104.1075 : 0.569:+	$C_5H_{14}NO$	104.1075	0.0	Choline	HMDB0000097	2	12.54
Urine	106.0499 : 0.844:+	$C_3H_7NO_3$	106.0498	0.9	Serine	HMDB0000187	2	11.45
Urine	118.0863 : 0.958:+	$C_5H_{11}NO_2$	118.0862	0.8	Betaine	HMDB0000043	2	12.35
Urine	133.0611 : 0.885:+	$C_4H_8N_2O_3$	133.0607	3.0	Asparagine	HMDB0000168	2	12.87
Urine	137.0460 : 1.067:+	$C_5H_4N_4O$	137.0458	1.5	Hypoxanthine	HMDB0000157	2	6.33
Urine	137.0706 : 0.613:+	$C_7H_8N_2O$	137.0709	2.2	Methylnicotinamide	HMDB0003152	2	16.81
Urine	138.0550 : 0.891:+	$C_7H_7NO_2$	138.0549	0.7	*p*-Aminobenzoic acid	HMDB0001392	2	13.31
Urine	141.0660 : 0.690:+	$C_6H_8N_2O_2$	141.0658	1.4	Imidazole propionic acid	HMDB0002820	2	8.23
Urine	144.1020 : 0.967:+	$C_7H_{13}NO_2$	144.1019	0.7	Proline betaine	HMDB0004827	1	12.88
Urine	146.0812 : 1.183:+	$C_6H_{11}NO_3$	146.0811	0.7	*Unknown*	HMDB0001263	4	9.13
Urine	147.0764 : 0.911:+	$C_5H_{10}N_2O_3$	147.0764	0.0	Glutamine	HMDB0000641	2	8.92
Urine	147.1128 : 0.583:+	$C_6H_{14}N_2O_2$	147.1128	0.0	Lysine	HMDB0000182	2	9.50
Urine	148.0604 : 0.924:+	$C_5H_9NO_4$	148.0604	0.0	Glutamic acid	HMDB0003339	2	11.26
Urine	150.0775 : 0.844:+	$C_6H_7N_5$	150.0774	0.7	*Unknown*		4	25.74
Urine	156.0768 : 0.620:+	$C_6H_9N_3O_2$	156.0767	0.6	Histidine	HMDB0000177	2	6.84
Urine	160.0970 : 1.089:+	$C_7H_{13}NO_3$	160.0968	1.2	*Unknown*		2	9.27
Urine	162.1125 : 0.714:+	$C_7H_{15}NO_3$	162.1124	0.6	Carnitine	HMDB0000062	2	9.60
Urine	166.0724 : 0.702:+	$C_6H_7N_5O$	166.0723	0.6	Methylguanine	HMDB0001566	2	8.66

Urine	170.0924 : 0.634:+	$C_7H_{11}N_3O_2$	170.0924	0.0	3-Methylhistidine	HMDB0000479	1	6.14
Urine	175.1190 : 0.602:+	$C_6H_{14}N_4O_2$	175.1189	0.6	Arginine	HMDB0000517	2	8.53
Urine	176.0666 : 0.851:+	$C_5H_9N_3O_4$	176.0666	0.0	Guanidinosuccinic acid	HMDB0003157	2	5.62
Urine	176.1030 : 0.772:+	$C_6H_{13}N_3O_3$	176.1029	0.6	Citrulline	HMDB0000904	2	6.46
Urine	182.0810 : 0.957:+	$C_9H_{11}NO_3$	182.0811	0.5	Tyrosine	HMDB0000158	2	9.86
Urine	189.1598 : 0.603:+	$C_9H_{20}N_2O_2$	189.1597	0.5	Trimethyllysine	HMDB0001325	2	14.16
Urine	204.1230 : 0.758:+	$C_9H_{17}NO_4$	204.123	0.0	Acetylcarnitine	HMDB0000201	2	12.37
Urine	205.0972 : 0.924:+	$C_{11}H_{12}N_2O_2$	205.0971	0.5	Tryptophan	HMDB0000929	2	28.26
Urine	217.1560 : 0.847:+	$C_{10}H_{21}N_2O_3$	217.1546	6.4	Valylvaline	HMDB0029140	2	25.92
Urine	232.1544 : 0.794:+	$C_{11}H_{21}NO_4$	232.1543	0.4	Butyrylcarnitine	HMDB0002013	2	10.77
Urine	260.1495 : 0.817:+	$C_{12}H_{21}NO_5$	260.1492	1.2	*Unknown*		4	16.33
Urine	276.1441 : 0.858:+	$C_{12}H_{21}NO_6$	276.1441	0.0	Glutarylcarnitine	HMDB0013130	2	7.71
Urine	286.2013 : 0.861:+	$C_{15}H_{27}NO_4$	286.2013	0.0	*Unknown*		4	9.81
Urine	367.1509 : 1.084:+	$C_{17}H_{22}N_2O_7$	367.15	2.5	Mannosyltryptophan		2	6.60
Urine	487.2120 : 0.825:+	$C_{18}H_{34}N_2O_{13}$	487.2134	2.9	Glucosylgalactosyl hydroxylysine	HMDB0000585	2	8.54
Urine	89.0244 : 1.534:-	$C_3H_6O_3$	89.0243	1.1	Lactic acid	HMDB0000190	2	27.69
Urine	105.0193 : 1.488:-	$C_3H_6O_4$	105.0193	0.0	Glycerate	HMDB0000139	2	21.65
Urine	121.0295 : 1.142:-	$C_7H_6O_2$	121.0294	0.8	Benzoic acid	HMDB0001870	2	11.25
Urine	124.9914 : 1.663:-	$C_2H_6O_4S$	124.9913	0.8	Ethylsulfate	HMDB0031233	2	14.32
Urine	128.0353 : 1.345:-	$C_5H_7NO_3$	128.0352	0.8	Oxo-proline	HMDB0000267	2	14.51
Urine	135.0299 : 1.306:-	$C_4H_8O_5$	135.0298	0.7	Threonic acid	HMDB62620	2	14.99
Urine	144.0458 : 1.192:-	C_9H_7NO	144.0454	2.8	Indole-3-carboxaldehyde	HMDB0029737	2	19.91
Urine	146.0460 : 1.972:-	$C_5H_9NO_4$	146.0458	1.4	Glutamic acid	HMDB0000148	2	13.12
Urine	153.0193 : 1.576:-	$C_7H_6O_4$	153.0193	0.0	Dihydroxybenzoic acid	HMDB0013677	2	16.22

Urine	161.9869 : 1.561:-	$C_4H_5NO_4S$	161.9866	1.9	Acesulfame K	HMDB0033585	1	25.13
Urine	167.0211 : 1.257:-	$C_5H_4N_4O_3$	167.021	0.6	Uric acid	HMDB0000289	2	12.41
Urine	171.0068 : 1.755:-	$C_3H_9O_6P$	171.0063	2.9	Glycerol phosphate	HMDB0002520	2	8.54
Urine	177.0229 : 1.180:-	$C_6H_{10}O_4S$	177.0226	1.7	*Unknown*		4	26.13
Urine	178.0510 : 1.176:-	$C_9H_9NO_3$	178.0509	0.6	Hippuric acid	HMDB0000714	2	22.57
Urine	181.9917 : 1.463:-	$C_7H_5NO_3S$	181.9917	0.0	Saccharin	HMDB0029723	1	8.38
Urine	182.0459 : 1.221:-	$C_8H_9NO_4$	182.0458	0.5	Pyridoxic acid	HMDB0000017	2	16.91
Urine	185.0820 : 1.781:-	$C_9H_{14}O_4$	185.0819	0.5	*Unknown*		4	18.92
Urine	187.0071 : 1.416:-	$C_7H_8O_4S$	187.007	0.5	*p*-Cresol sulfate	HMDB0011635	2	14.36
Urine	188.9865 : 1.444:-	$C_6H_6O_5S$	188.9862	1.6	Pyrocatechnol sulfate	HMDB0059724	2	32.92
Urine	191.0552 : 1.142:-	$C_7H_{12}O_6$	191.056	4.2	Quinic acid	HMDB0003072	2	13.44
Urine	193.0373 : 1.122:-	$C_7H_6N_4O_3$	193.0366	3.6	*Unknown*		4	13.12
Urine	212.0023 : 1.357:-	$C_8H_7NO_4S$	212.0022	0.5	Indoxyl sulfate	HMDB0000682	2	12.04
Urine	225.0631 : 1.089:-	$C_8H_{10}N_4O_4$	225.0629	0.9	5-Acetylamino-6-formylamino-3-methyluracil	HMDB0011105	2	21.23
Urine	238.0780 : 1.505:-				*Unknown* $[M-2H]^{2-}$		4	14.49
Urine	263.1037 : 1.037:-	$C_{13}H_{16}N_2O_4$	263.1037	0.0	Phenylacetylglutamine	HMDB0006344	2	12.07
Urine	283.0827 : 1.012:-	$C_{13}H_{16}O_7$	283.0823	1.4	*p*-Cresol glucuronide	HMDB0011686	2	13.97
Urine	287.0236 : 1.152:-	$C_{11}H_{12}O_7S$	287.023	2.1	Dihydroxyphenyl-γ-valerolactone sulfate	HMDB0029191	2	26.79
Urine	302.1138 : 1.016:-	$C_{15}H_{17}N_3O_4$	302.1146	2.6	Indoleacetyl glutamine	HMDB0013240	2	7.79
Urine	308.0987 : 0.984:-	$C_{11}H_{19}NO_9$	308.0987	0.0	*Unknown*		4	12.74
Urine	331.1760 : 0.964:-	$C_{17}H_{24}N_4O_3$	331.1776	4.8	*Unknown*		4	10.67
Urine	377.0170 : 1.040:-	$C_{17}H_6N_4O_7$	377.0164	1.6	*Unknown*		4	20.45
Urine	473.1453 : 0.934:-	$C_{24}H_{25}O_{l0}$	473.1448	1.1	Enterolactone glucuronide	--	2	14.37
Urine	632.2044 : 0.874:-	$C_{23}H_{39}NO_{19}$	632.2043	0.2	Sialyllactose	HMDB0000825	2	9.78

Urine	112.0515 : 0.710:-	$C_4H_7N_3O$	112.0516	0.9	Creatinine	HMDB0000562	2	9.61
Plasma	76.0402 : 0.732:+	$C_2H_5NO_2$	76.0393	11.8	Glycine	HMDB0000123	2	8.17
Plasma	90.0557 : 0.783:+	$C_3H_7NO_2$	90.0549	8.9	Alanine	HMDB0000161	2	4.15
Plasma	104.1075 : 0.592:+	$C_5H_{14}NO$	104.1075	0.0	Choline	HMDB0000097	2	30.39
Plasma	106.0500 : 0.864:+	$C_3H_7NO_3$	106.0498	1.9	Serine	HMDB0000187	2	3.23
Plasma	114.0662 : 0.635:+	$C_4H_7N_3O$	114.0653	7.9	Creatinine	HMDB0000562	2	32.14
Plasma	116.0705 : 0.927:+	$C_5H_9NO_2$	116.0706	0.9	Proline	HMDB0000162	2	3.55
Plasma	118.0618 : 0.718:+	$C_3H_7N_3O_2$	118.0611	5.9	Guanidoacetic acid	HMDB0000128	2	9.93
Plasma	120.0654 : 0.900:+	$C_4H_9NO_3$	120.0655	0.8	Threonine	HMDB0000167	2	8.14
Plasma	129.0656 : 0.75:+	$C_5H_8N_2O_2$	129.0658	1.5	*Unknown*		3	6.84
Plasma	132.0766 : 0.765:+	$C_4H_9N_3O_2$	132.0767	0.8	Creatine	HMDB0000064	2	4.80
Plasma	132.1017 : 0.873:+	$C_6H_{13}NO_2$	132.1019	1.5	Leucine/isoleucine	HMDB0000687	2	5.20
Plasma	133.0573 : 0.901:+	$C_4H_8N_2O_3$	133.0607	25.6	Asparagine	HMDB0000168	2	4.20
Plasma	137.0459 : 1.066:+	$C_5H_4N_4O$	137.0458	0.7	Hypoxanthine	HMDB0000157	2	12.85
Plasma	144.0988 : 0.984:+	$C_7H_{13}NO_2$	144.1013	17.3	Proline betaine	HMDB0004827	2	45.39
Plasma	146.1182 : 0.699:+	$C_7H_{15}NO_2$	146.1176	4.1	Deoxycarnitine	HMDB0001161	3	26.48
Plasma	147.0761 : 0.922:+	$C_5H_{10}N_2O_3$	147.0763	1.4	Glutamine	HMDB0000641	2	3.81
Plasma	148.0603 : 0.934:+	$C_5H_9NO_4$	148.0603	0.0	Glutamic acid	HMDB0003339	2	8.50
Plasma	150.0583 : 0.910:+	$C_5H_{11}NO_2S$	150.0583	0.0	Methionine	HMDB0000696	2	4.65
Plasma	152.0567 : 0.910:+	$C_5H_5N_5O$	152.0563	2.6	Guanine	HMDB0000132	2	34.61
Plasma	156.0766 : 0.649:+	$C_6H_9N_3O_2$	156.0763	1.9	Histidine	HMDB0000177	2	31.32
Plasma	160.1332 : 0.725:+	$C_8H_{17}NO_2$	160.1323	5.6	2-Aminooctanoic acid	HMDB0000991	2	22.11
Plasma	162.0761 : 0.933:+	$C_6H_{11}NO_4$	162.0753	4.9	Aminoadipic acid	HMDB0000510	2	14.34
Plasma	162.1123 : 0.735:+	$C_7H_{15}NO_3$	162.1123	0.0	Carnitine	HMDB0000062	2	3.89
Plasma	166.086 : 0.9355:+	$C_9H_{11}NO_2$	166.0853	4.2	Phenylalanine	HMDB0000159	2	12.34

Plasma	170.0922 : 0.663:+	$C_7H_{11}N_3O_2$	170.0923	0.6	Methylhistidine	HMDB0000479	2	15.47
Plasma	175.1191 : 0.631:+	$C_6H_{14}N_4O_2$	175.1183	4.6	Arginine	HMDB0000517	2	37.36
Plasma	176.1025 : 0.943:+	$C_6H_{13}N_3O_3$	176.1023	1.1	Citrulline	HMDB0000904	2	4.25
Plasma	182.081 : 0.9616:+	$C_9H_{11}NO_3$	182.0803	3.8	Tyrosine	HMDB0000158	2	3.52
Plasma	189.1337 : 0.635:+	$C_7H_{16}N_4O_2$	189.1343	3.2	Monomethylarginine	HMDB0029416	2	44.31
Plasma	202.1807 : 0.793:+	$C_{11}H_{23}NO_2$	202.1802	2.5	*Unknown*		4	56.73
Plasma	203.1499 : 0.680:+	$C_8H_{18}N_4O_2$	203.1493	3.0	Dimethylarginine	HMDB0003334/ HMDB0001539	2	11.69
Plasma	204.1233 : 0.776:+	$C_9H_{17}NO_4$	204.1223	4.9	Acetylcarnitine	HMDB0000201	2	4.50
Plasma	205.0966 : 0.931:+	$C_{11}H_{12}N_2O_2$	205.0963	1.5	Tryptophan	HMDB0000929	2	17.46
Plasma	241.0289 : 0.950:+	$C_6H_{12}N_2O_4S_2$	241.0303	5.8	Cystine (disulfide)	HMDB0000192	2	5.04
Plasma	247.1441 : 1.146:+	$C_{14}H_{18}N_2O_2$	247.1433	3.2	Tryptophan betaine	HMDB0061115	2	14.53
Plasma	298.0526 : 0.823:+	$C_8H_{15}N_3O_5S_2$	298.0523	1.0	Cysteinylglycine disulfide	HMDB0000709	2	7.87
Plasma	87.0087 : 1.301:-	$C_3H_4O_3$	87.00874	0.5	Pyruvic acid	HMDB0000243	2	14.14
Plasma	89.0244 : 1.136:-	$C_3H_6O_3$	89.02439	0.1	Lactic acid	HMDB0000190	2	8.13
Plasma	103.0400 : 1.019:-	$C_4H_8O_3$	103.04	0.0	3-Hydroxybutyric acid	HMDB0000357	2	6.91
Plasma	103.0400 : 1.043:-	$C_4H_8O_3$	103.04	0.0	2-Hydroxybutyric acid	HMDB0000008	2	11.53
Plasma	115.0400 : 1.078:-	$C_5H_8O_3$	115.04	0.0	Alpha-ketoisovaleric acid	HMDB0000019	2	15.83
Plasma	117.0193 : 1.766:-	$C_4H_6O_4$	117.0193	0.0	Succinic acid	HMDB0000254	2	31.01
Plasma	128.0353 : 1.018:-	$C_5H_7NO_3$	128.0352	0.8	Oxo-proline	HMDB0000267	2	11.92
Plasma	129.0557 : 1.029:-	$C_6H_{10}O_3$	129.0556	0.8	3-methyl-2-oxovaleric acid	HMDB0000491	2	13.47
Plasma	132.0302 : 1.073:-	$C_4H_7NO_4$	132.0302	0.0	Aspartic acid	HMDB0006483	2	12.40
Plasma	133.0142 : 1.783:-	$C_4H_6O_5$	133.0142	0.0	Malic acid	HMDB0000744	2	32.51
Plasma	167.021 : 0.969:-	$C_5H_4N_4O_3$	167.021	0.0	Uric acid	HMDB0000289	2	11.10
Plasma	179.0561 : 0.999:-	$C_6H_{12}O_6$	179.056	0.6	Glucose	HMDB0000122	2	11.73

Plasma	191.0197 : 1.967:-	$C_6H_8O_7$	191.0197	0.0	Citric acid	HMDB0000094	2	21.51
Plasma	195.051 : 0.889:-	$C_6H_{12}O_7$	195.051	0.0	Gluconic acid	HMDB0000625	2	13.37
Plasma	C14:0 : 10.15	$C_{14}H_{28}O_2$			Myristic acid	HMDB0000806	2	19.55
Plasma	C15:0 : 10.79	$C_{15}H_{30}O_2$			Pentadecanoic acid	HMDB0000826	2	13.63
Plasma	C16:0 : 11.43	$C_{16}H_{32}O_2$			Palmitic acid	HMDB0000220	2	12.70
Plasma	C16:1 1 : 11.74	$C_{16}H_{30}O_2$			Hexadecenoic acid	HMDB0037647	2	13.16
Plasma	C16:1 2 : 11.82	$C_{16}H_{30}O_2$			Palmitoleic acid	HMDB0003229	2	14.46
Plasma	C17:0 : 12.06	$C_{17}H_{34}O_2$			Margaric acid	HMDB0002259	2	12.27
Plasma	C18:0 : 12.77	$C_{18}H_{36}O_2$			Stearic acid	HMDB0000827	2	13.24
Plasma	C18:1 1 : 13.20	$C_{18}H_{34}O_2$			Elaidic acid	HMDB0000573	2	11.85
Plasma	C18:1 2 : 13.26	$C_{18}H_{34}O_2$			Oleic acid	HMDB0000207	2	8.50
Plasma	C18:2 1 : 13.92	$C_{18}H_{32}O_2$			Linoleic acid	HMDB0000673	2	13.94
Plasma	C18:2 2 : 15.02	$C_{18}H_{32}O_2$			Linoelaidic acid	HMDB0006270	2	33.45
Plasma	C18:3 1 : 14.47	$C_{18}H_{30}O_2$			γ-Linolenic acid	HMDB0003073	2	17.16
Plasma	C18:3 2 : 14.82	$C_{18}H_{30}O_2$			α-Linolenic acid	HMDB0001388	2	14.86
Plasma	C20:0 : 14.37	$C_{20}H_{40}O_2$			Arachidic acid	HMDB0002212	2	13.34
Plasma	C20:1 : 14.88	$C_{20}H_{38}O_2$			Eicosenoic acid	HMDB0002231	2	30.24
Plasma	C20:2 : 15.75	$C_{20}H_{36}O_2$			Eicosadienoic acid	HMDB0005060	2	19.19
Plasma	C20:3 1 : 16.41	$C_{20}H_{34}O_2$			Eicosatrienoic acid	HMDB0002925	2	11.94
Plasma	C20:3 2 : 17.44	$C_{20}H_{34}O_2$			Unknown		4	18.70
Plasma	C20:4 : 16.94	$C_{20}H_{32}O_2$			Arachidonic acid	HMDB0001043	2	13.71
Plasma	C20:5 : 18.18	$C_{20}H_{30}O_2$			Eicosapentaenoic acid	HMDB0001999	2	17.27
Plasma	C22:0 : 16.34	$C_{22}H_{44}O_2$			Behenic acid	HMDB0000944	2	13.57
Plasma	C22:5 1 : 19.43	$C_{22}H_{34}O_2$			*Unknown*		4	13.76
Plasma	C22:5 2 : 20.8	$C_{22}H_{34}O_2$			Docosapentaenoic	HMDB0006528	2	14.12

Plasma	C22:6 : 21.34	$C_{22}H_{32}O_2$	Docosahexaenoic acid	HMDB0062579	2	12.88
Plasma	C24:0 : 18.63	$C_{24}H_{48}O_2$	Lignoceric acid	HMDB0002003	2	12.15
Plasma	C24:1 :19.28	$C_{24}H_{46}O_2$	Nervonic acid	HMDB0002368	2	10.88

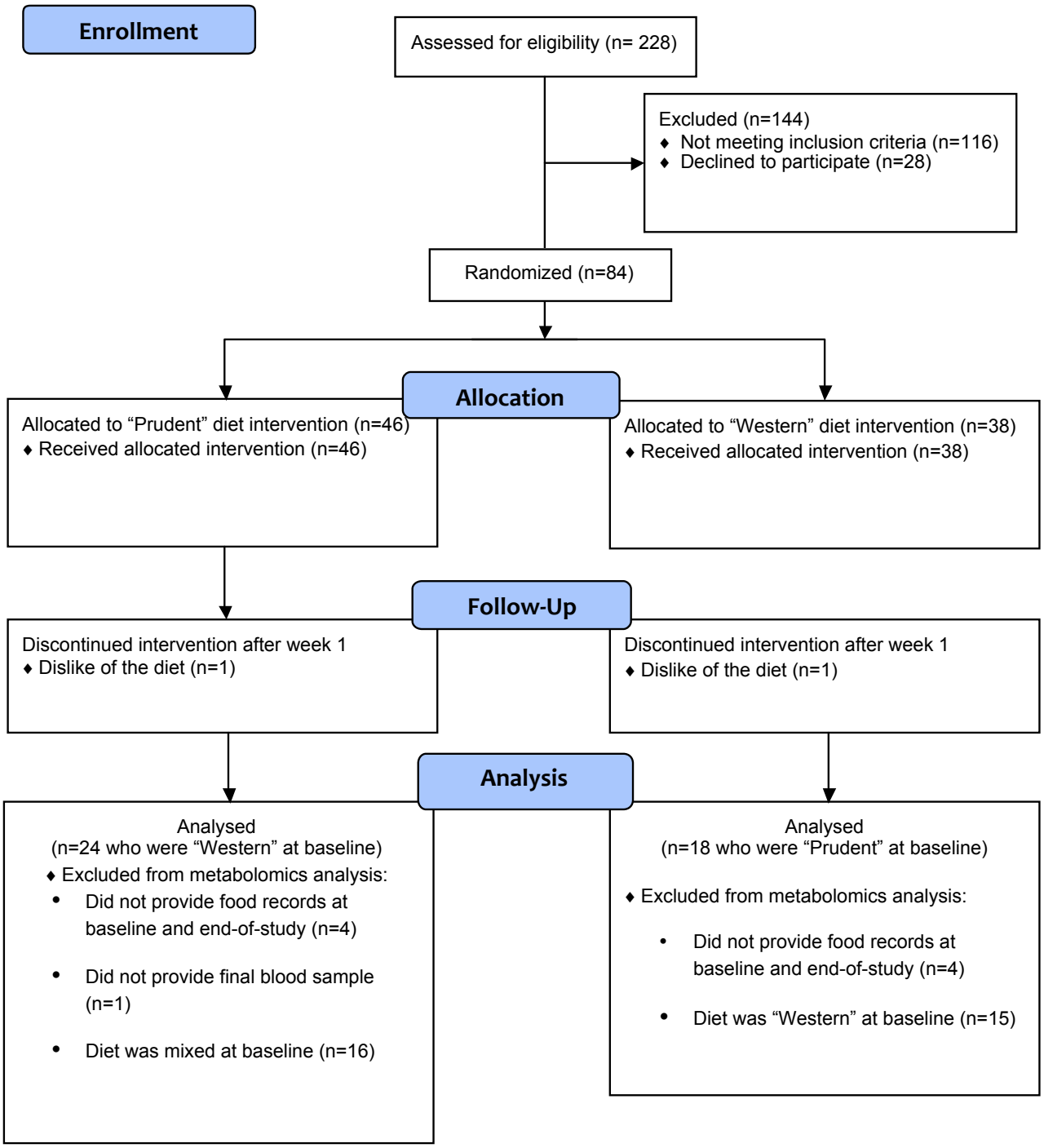

Figure S1. A CONCERT flow diagram outlining selection criteria used in a parallel two-arm randomized clinical trial involving participants from the DIGEST study, where metabolomic analyses was performed unblinded on paired serum and urine samples collected at baseline and 2 weeks following a provisional Prudent or Western diet. Overall, 73 of the 84 participants who completed DIGEST had available specimens and complete food records. However, in order to maximize the effect size of this short-term dietary intervention, metabolomic analyses was performed only on a subset of participants (n=42) who had contrasting habitual diets at baseline as evaluated based on an aggregate diet quality score.

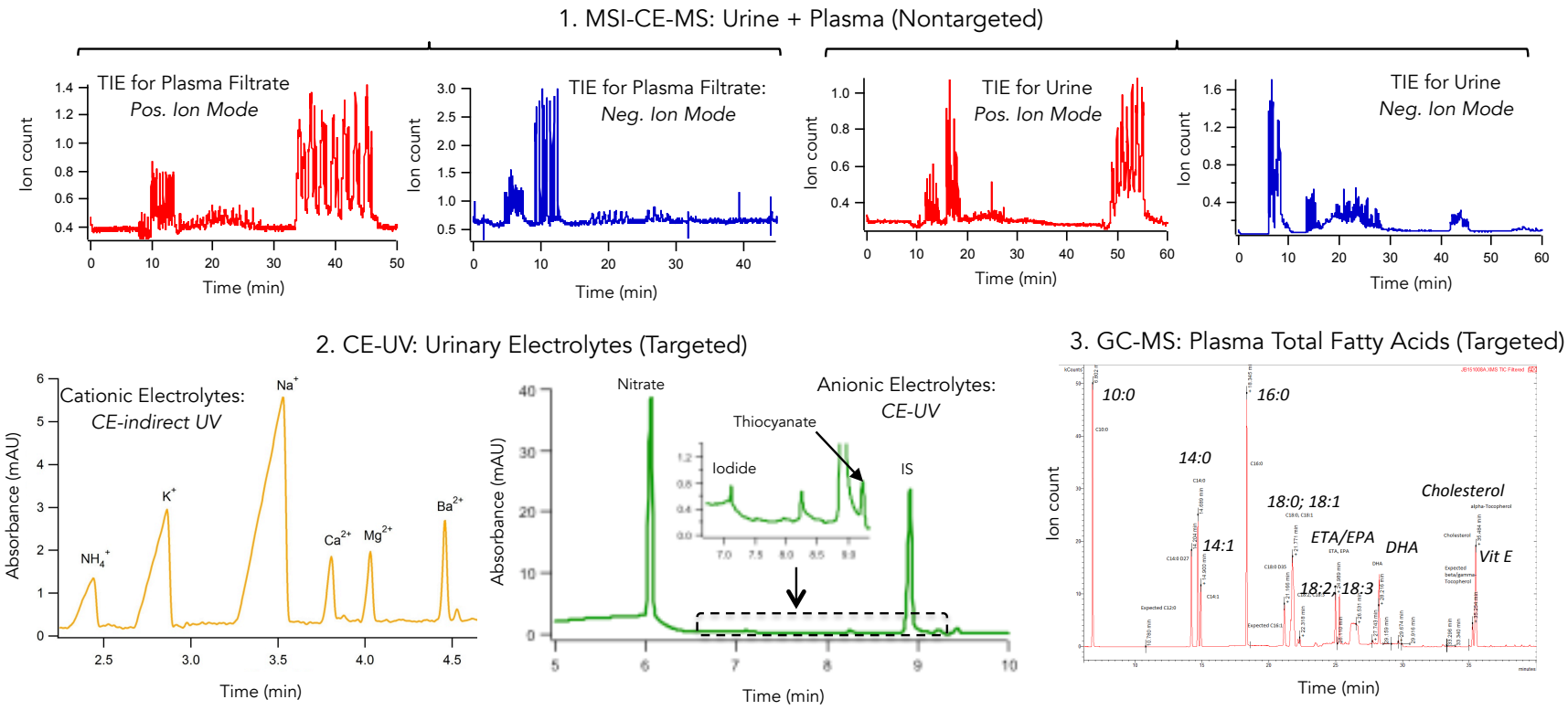

Figure S2. Overview of three major analytical platforms for nontargeted and targeted metabolite/electrolyte profiling of matching plasma and urine specimens from DIGEST participants at baseline and 2 weeks following an assigned Prudent or Western diet from food provisions. MSI-CE-MS was used as the major format for metabolomic analyses of a wide range of polar/ionic metabolites from both plasma filtrate and diluted urine samples when using a strigent data workflow for metabolite authentication with quality control. Also, CE with (indirect/direct) UV absorbance detection was used for targeted analysis of electrolytes in urine, including inorganic cations (*e.g.,* sodium) and anions (*e.g.,* nitrate), whereas GC-MS was applied for targeted analysis of total (hydrolyzed) fatty acids as their FAMEs from plasma extracts.

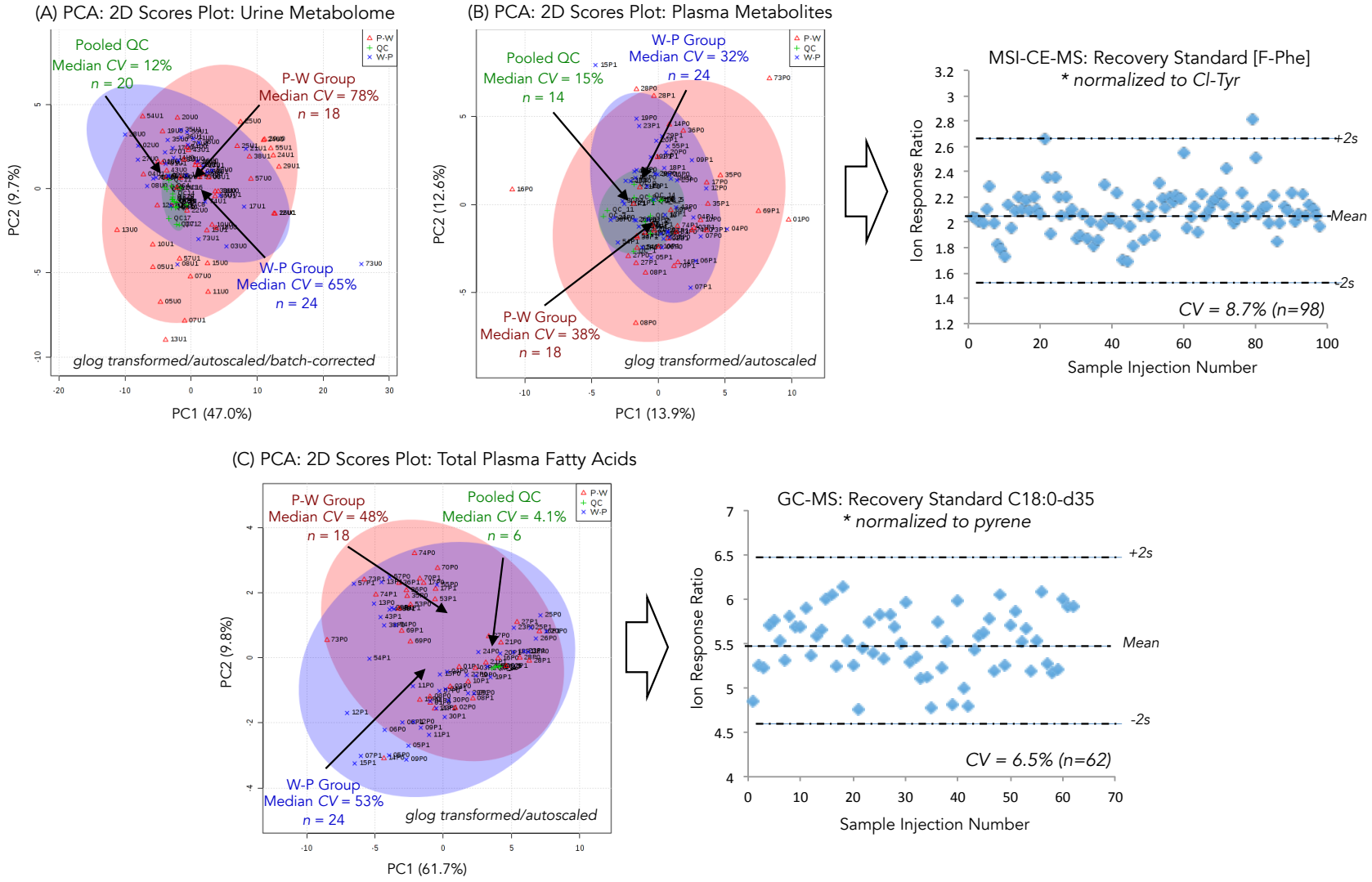

Figure S3. 2D scores plots from PCA and control charts for recovery standards that highlight the good technical precision as compared to biological variance of metabolomic data from three insturmental platforms, including (C) 84 authenticated metabolites in urine after QC-based batch-correction, (B) 80 polar/ionic metabolites from plasma using MSI-CE-MS and (C) 18 plasma (total) fatty acids using GC-MS.

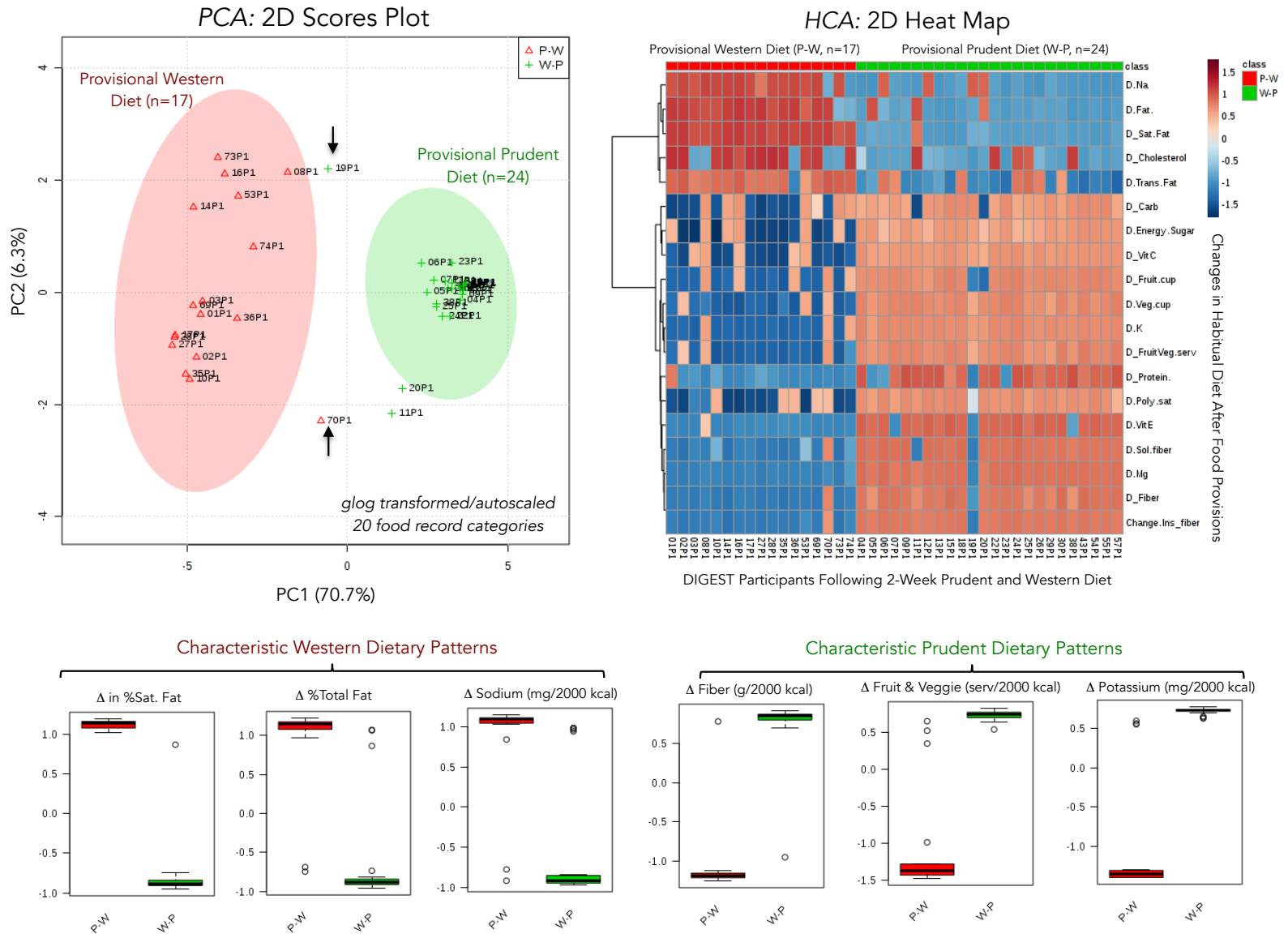

Figure S4. 2D scores plot from PCA and HCA/heat map summarizing changes in habitual diet (W-P and P-W) based on 20 macro-/micronutrient categories self-reported food records from DIGEST participants following 2 weeks of contrasting food provisions as compared to their baseline diet.

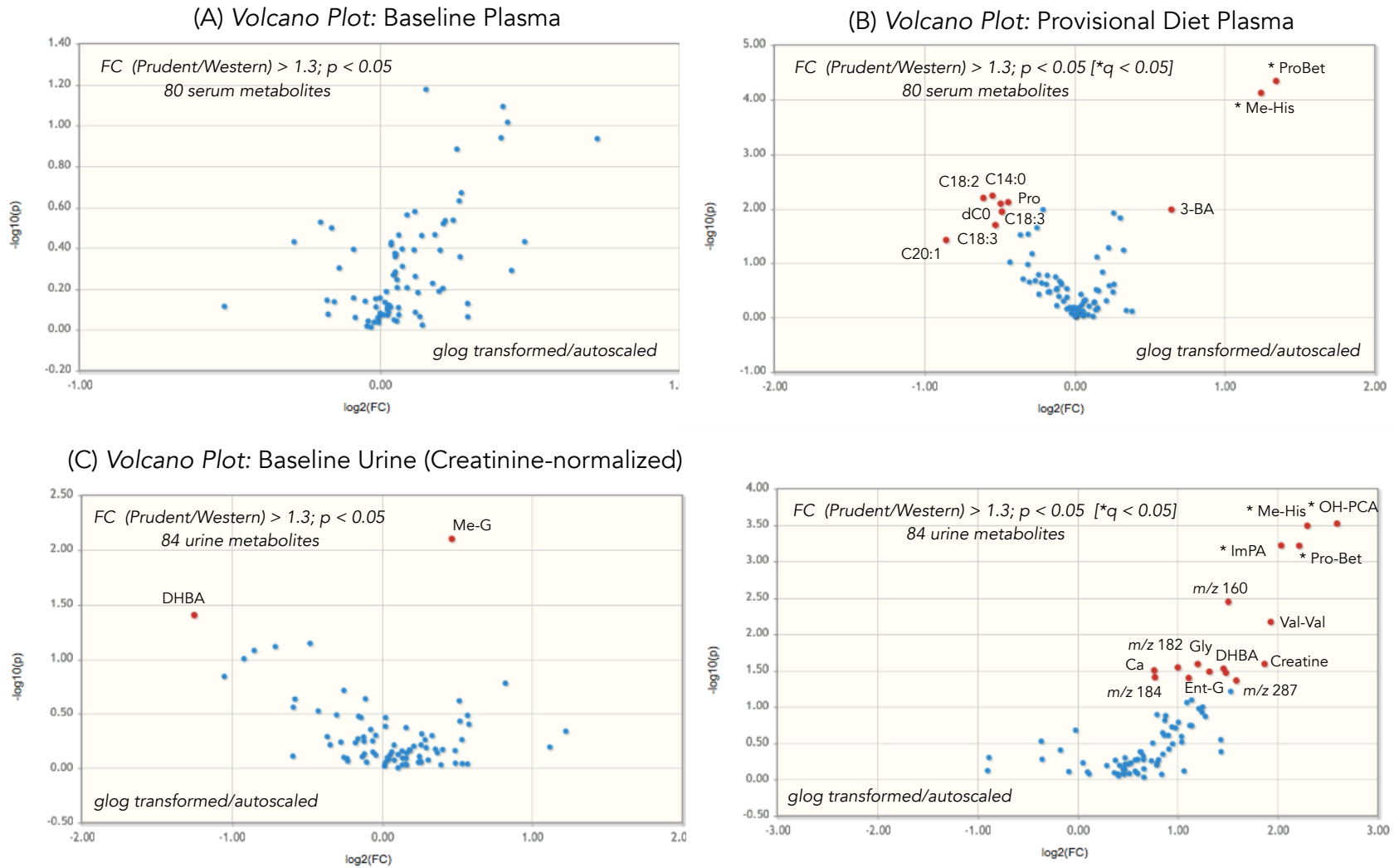

Figure S5. Series of volcano plots for urine (A, C) and plasma (B, D) metabolome data highlighting few differences in the metabolic phenotype among DIGEST participants (n=42) at baseline as compared to major changes following two weeks of contrasting diets from food provisions based on a minimum threshold for significance (mean $FC > 1.3$, $p < 0.05$) between Prudent and Western assigned groups (mean $FC > 1.3$ and $p < 0.05$). Abbreviations refer to DHBA (dihydroxybenzoic acid), ProBet (proline betaine), Me-His (3-methylhistidine), 3-OH-BA (3-hydroxybutyric acid), dC0 (deoxycarnitine), Pro (proline), OH-PCA (hydroxypipecolic acid), ImPA (imidazolepropionic acid), Ent-G (enterolactone glucuronide), DHBA (dihydroxybenzoic acid) and Me-G (methylguanine), whereas standard notation are used for plasma fatty acids and unknown ions denoted by their accurate mass (m/z).

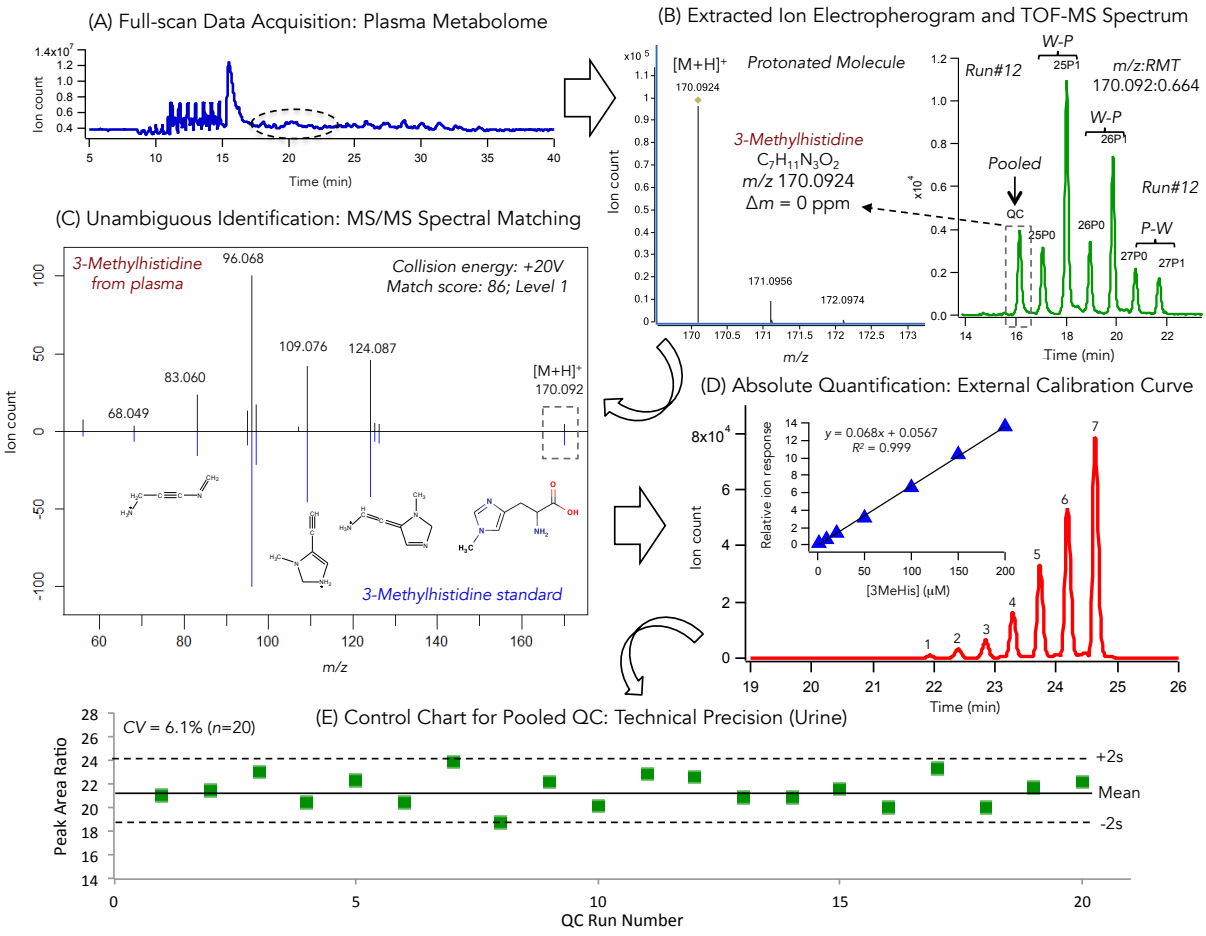

Figure S6. (A) Metabolomics data workflow for the identification and quantification of biomarkers of a provisional Prudent diet (*e.g.,* 3-methylhistidine annotated based on its *m/z*:RMT) when using full-scan data acquisition. (B) Multiplexed separations by MSI-CE-MS based on serial injection of seven plasma filtrate (or diluted urine) samples within a single run, including paired samples from each DIGEST participant (*i.e.,* baseline/post-treatment) together with a pooled sample as QC for assessing technical precision and long-term signal drift. High resolution MS under positive ion mode detection allows for determination of most likely molecular formula for unknown cation (*i.e.,* protonated molecular ion), whereas (C) MS/MS spectra is used for its structural elucidation when compared with an authentic standard. (D) Quantification for metabolites is then performed by external calibration when using an internal standard (Cl-Tyr) for data normalization by MSI-CE-MS. (E) A control chart for Me-His from pooled urine samples as QC analyzed in random positions in every run demonstrates acceptable technical precision over 3 days.

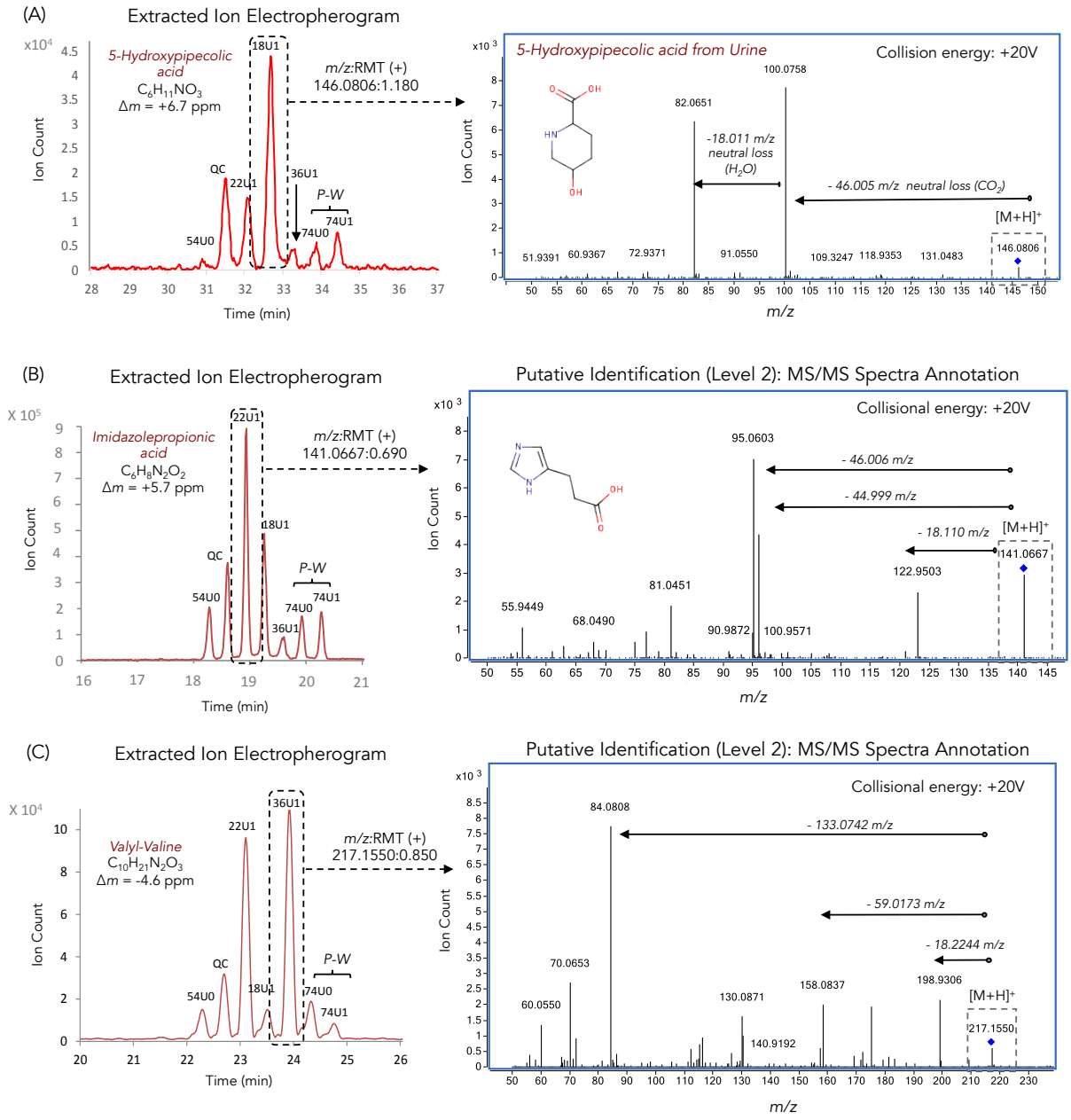

Figure S7. Putative identification (level 2) of three unknown cationic metabolites (MH^+) detected in urine specimens from DIGEST participants that were significantly elevated in assigned Prudent ($p < 0.05$) as compared to Western diet following 2 weeks of food provisions, namely (A) 5-hydroxypipecolic acid (OH-PCA, *m/z* 146.081), (B) imidazole propionic acid (ImPA, *m/z* 141.067) and (C) Valinyl-valine (Val-Val, *m/z* 217.155) based on their characteristic MS/MS spectra (optimal collision energy at 20 V) under positive ion mode conditions.

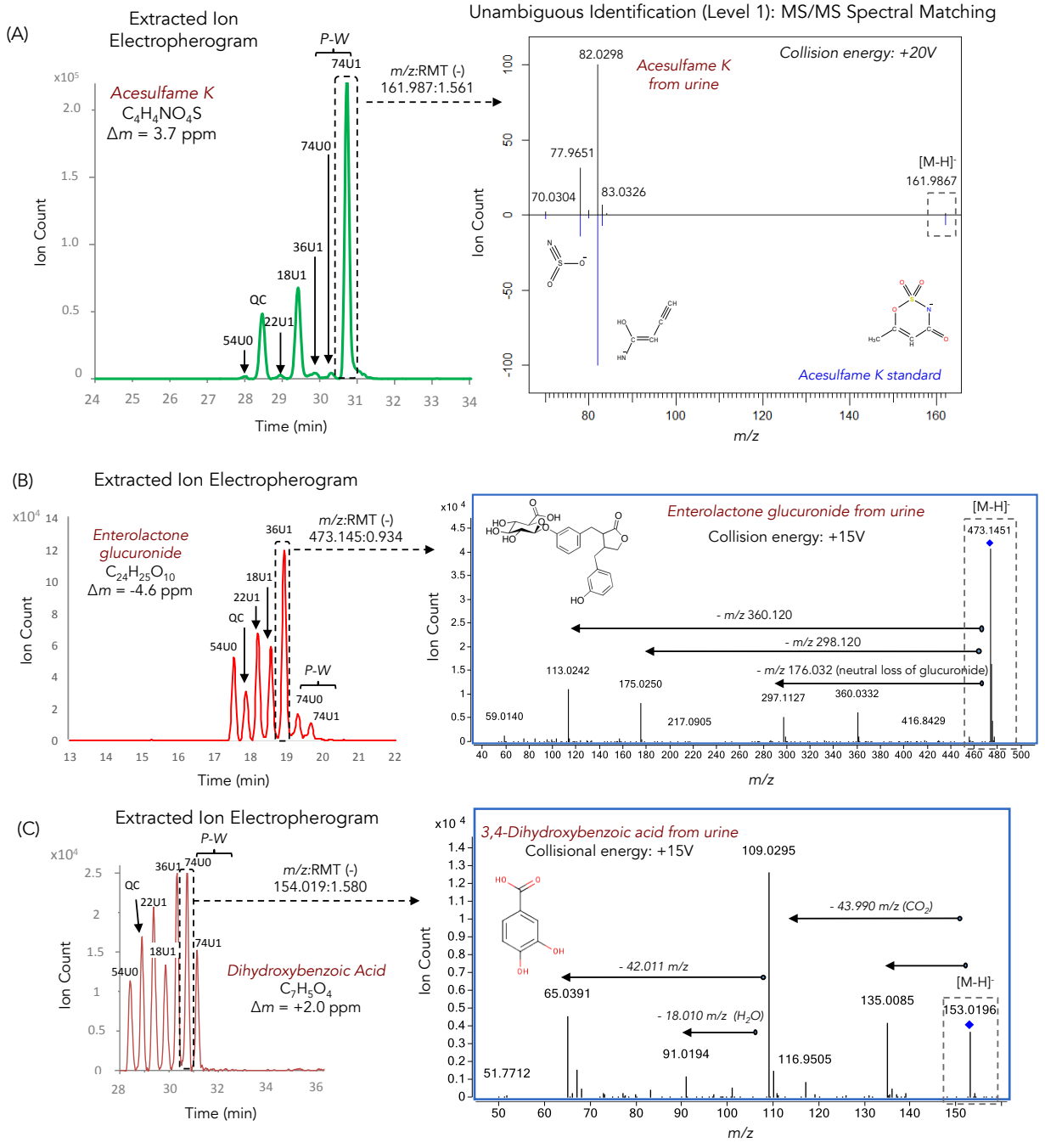

Figure S8. Unambiguous (level 1) and putative identification (level 2) of three unknown anionic metabolites ($M\text{-}H^-$) detected in urine specimens from DIGEST participants that were decreased (acesulfame K) or elevated (enterolactone glucuronide and dihydroxybenzoic acid) in assigned Prudent ($p < 0.05$) as compared to Western diet groups following 2 weeks of food provisions, namely (A) acesulfame K (ASK, *m/z* 161.987), (B) enterolactone glucuronide (Ent-G, *m/z* 473.145) and (C) dihydroxybenzoic acid (DHBA, *m/z* 153.020) based on their characteristic MS/MS spectra (optimal collision energies at 15 or 20 V) under negative ion mode conditions. Confident identification was derived from comparison of MS/MS spectra with a standard as shown in mirror plot for acesulfame K together with spiking into urine sample to confirm co-migration. The likely stereochemistry for DHBA was deduced from comparison of *in silico* MS/MS spectra when using HMDB, whereas Ent-G was tentatively identified based on comparison with published MS/MS spectra [Johnson et al. *Metabolites* **2013**, 3: 658-672].

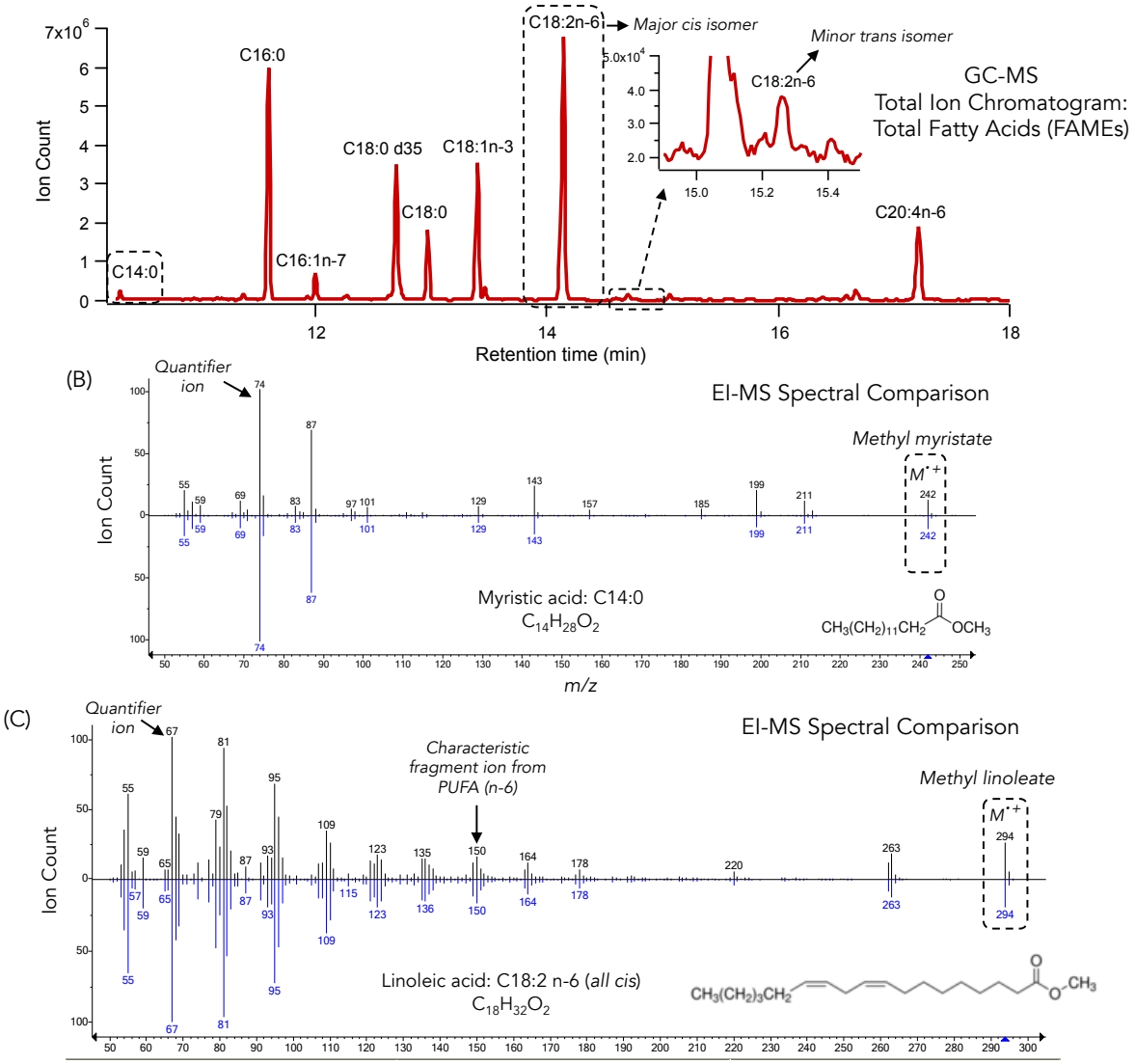

Figure S9. Unambiguous identification (level 1) of total (hydrolyzed) fatty acids as their FAME derivatives from plasma extracts when using GC-MS, including resolution of low abundance *trans*-isomer (linoelaidic acid, C18:2n-6*trans*) from major *cis*-isomer (linoleic acid, C18:2n-6*cis*), including detection of minor saturated fatty acids (myristic acid, C14:0). Mirror plots for EI-MS spectra show excellent matches when comparing FAMEs detected in plasma extracts as compared to their references in the NIST database, where the base peak ions correspond to the quantifier ions monitored for saturated and polyunsaturated fatty acids. Overall, plasma total C18:2n-6*cis* was only 0.34% of its major stereoisomer C18:2n-6*trans* that also represents the most abundant fatty acid measured in circulation.

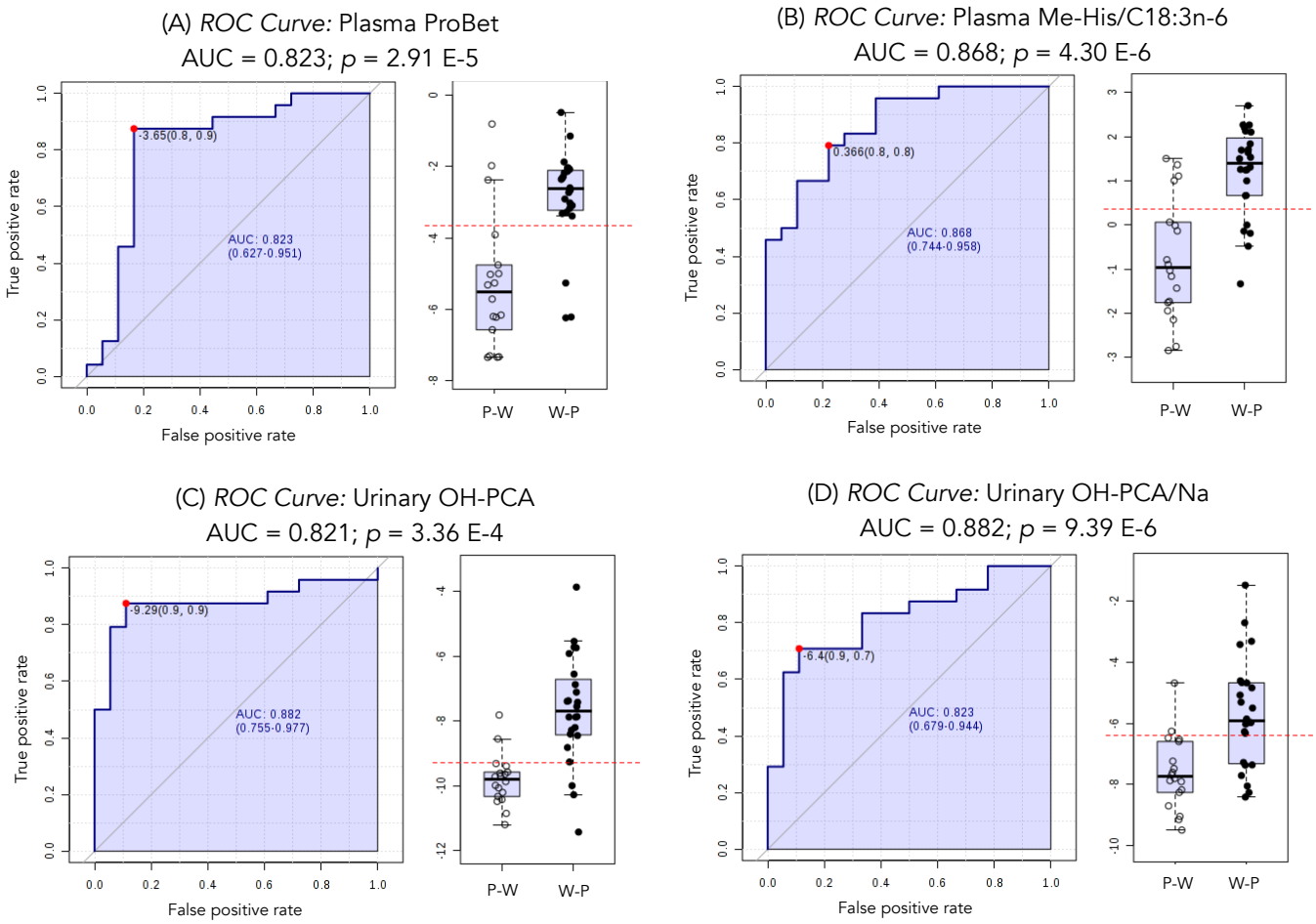

Figure S10. Top-ranked single and ratiometric metabolites for differentiation of DIGEST participants assigned a Prudent (W-P, *n*=24) or Western (P-W, n=18) diet following 2 weeks of food provisions when using receiver operating characteristic (ROC) curves. All metabolites were *glog*-transformed, whereas urine metabolites were normalized to creatinine following a QC-based batch correction. Overall, there was good discrimination of contrasting dietary patterns ($AUC > 0.820$; $p < 0.001$) as shown for (A) plasma proline betaine (ProBet), (B) plasma 3-methylhistidine to α-linoleic acid (MeHis/C18:3n-6) ratio, (C) urinary hydroxypipecolic acid (OH-PCA), and (D) urinary hydroxypipecolic acid to sodium ratio (OH-PCA/Na).

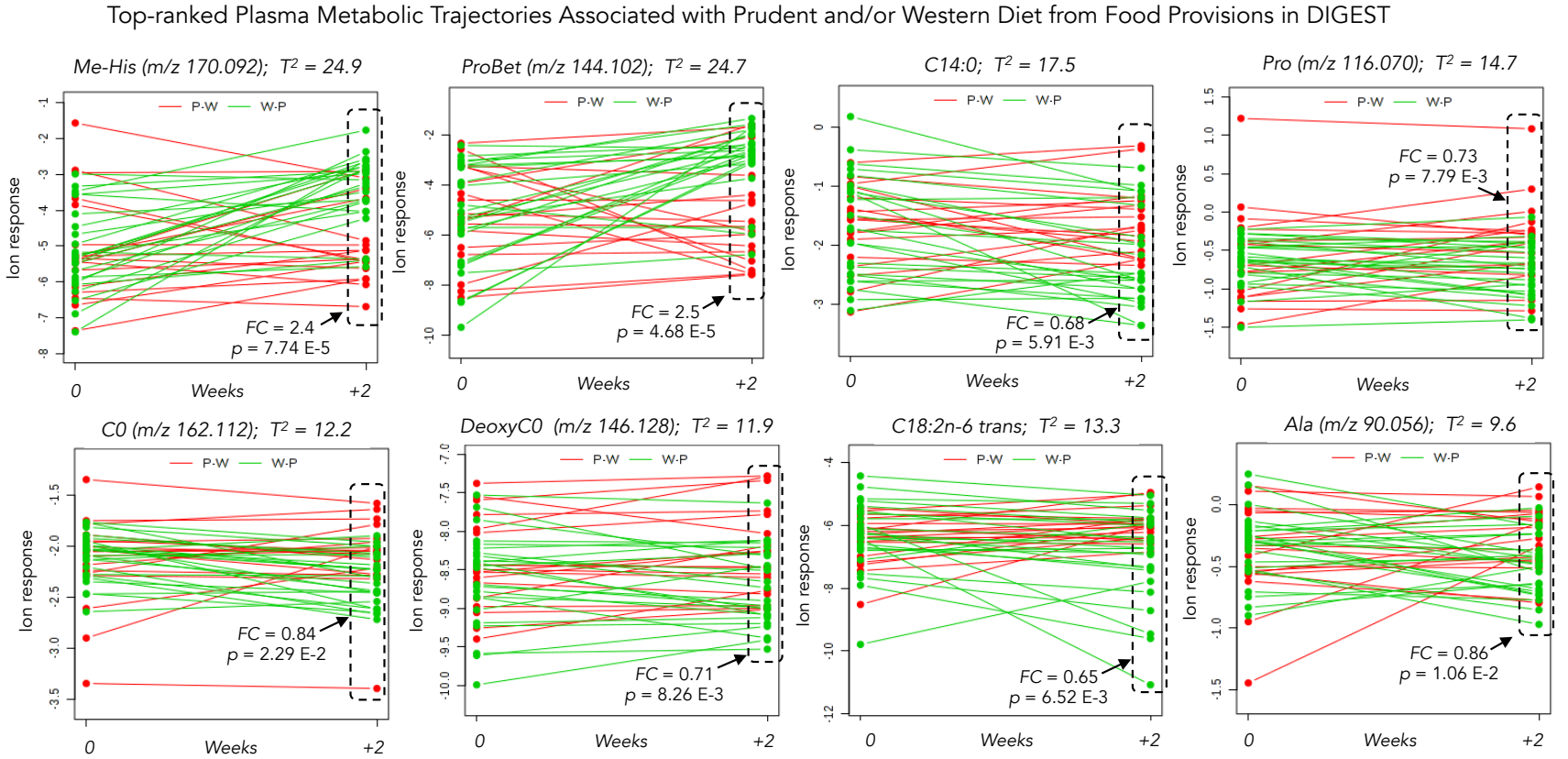

Figure S11. Top-ranked plasma metabolites associated with contrasting Prudent (W-P) and Western (P-W) diets from food provisions when using *glog*-transformed ion responses measured at baseline (habitual diet, 0) and following food provisions (2 weeks) for DIGEST participants (n=42). Metabolic trajectories from time course studies were ranked based on Hotelling-T^2 values when using multivariate empirical Bayes analysis of variance (MEBA) together with student's t-test to confirm statistical significance ($p < 0.05$) occurring after assigned diets as compared to baseline habitual diets ($p > 0.05$).

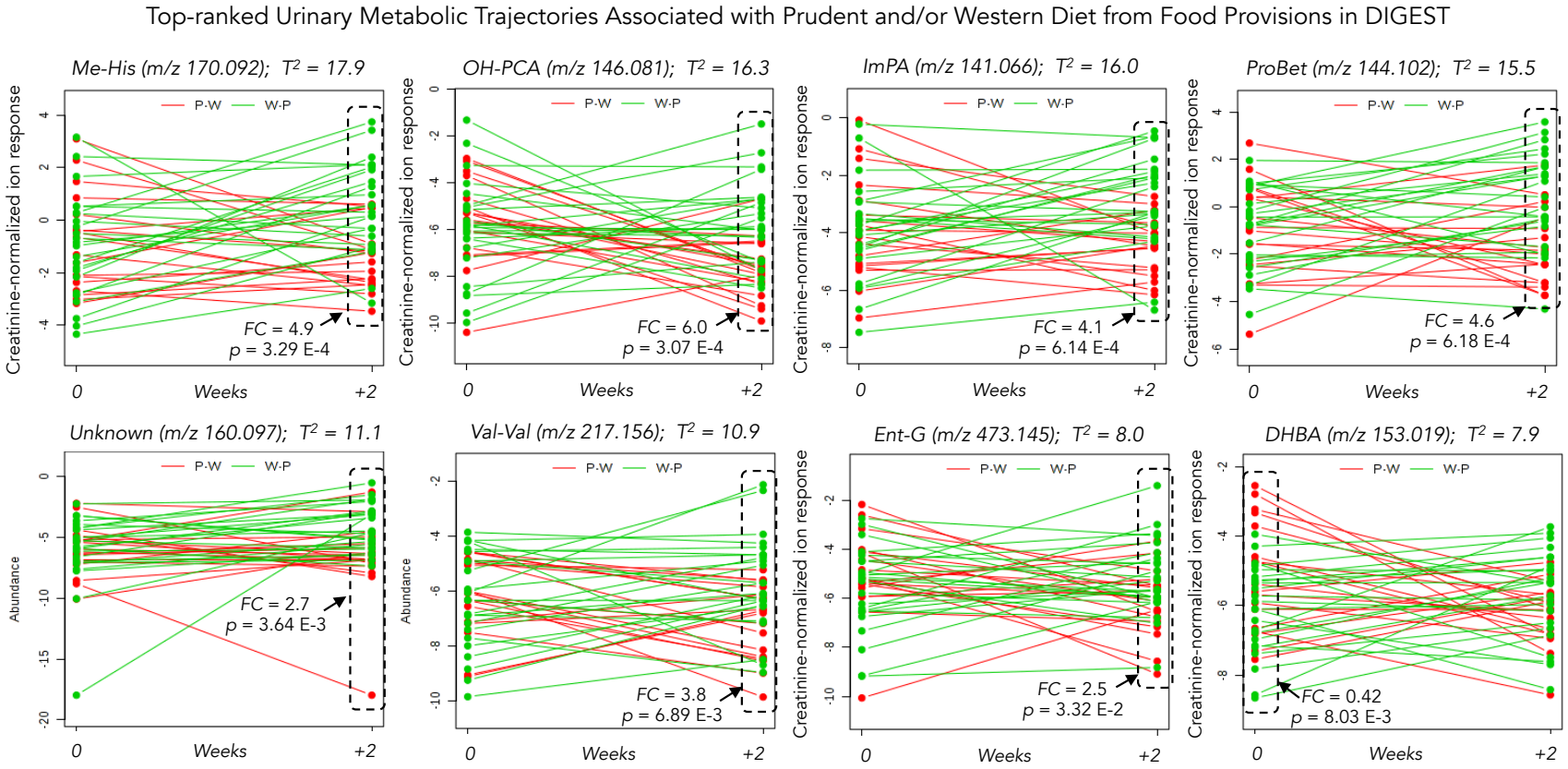

Figure S12. Top-ranked urinary metabolites associated with contrasting Prudent (W-P) and Western (P-W) diets from food provisions when using *glog*-transformed ion responses normalized to creatinine measured at baseline (habitual diet, 0) and following food provisions (2 weeks) for DIGEST participants (n=42). Metabolic trajectories from time course studies were ranked based on Hotelling-T^2 values when using multivariate empirical Bayes analysis of variance (MEBA) together with student's t-test to confirm statistical significance ($p < 0.05$) occurring after assigned diets as compared to baseline habitual diets ($p > 0.05$) with the exception for DHBA.

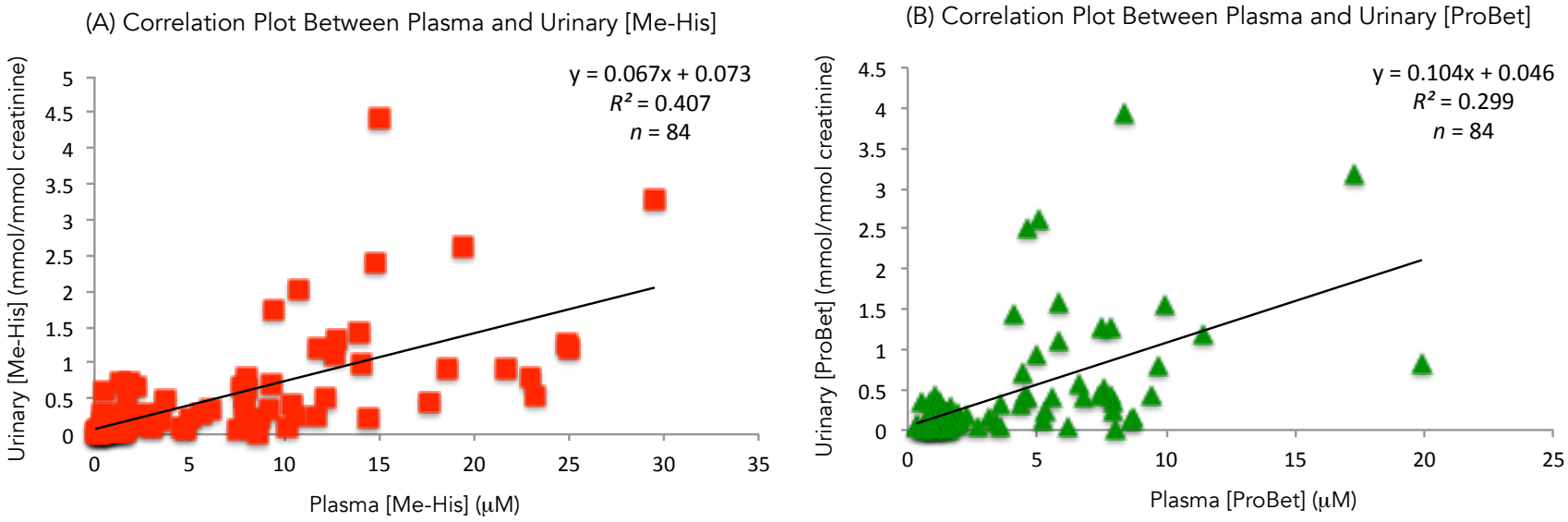

Figure S13. Linear correlation plots highlighting the strong association between fasting plasma concentrations of Me-His and ProBet and their creatinine-normalized concentrations measured independently from matching single-spot urine samples for DIGEST participants collected at baseline and then following 2 weeks of food provisions.

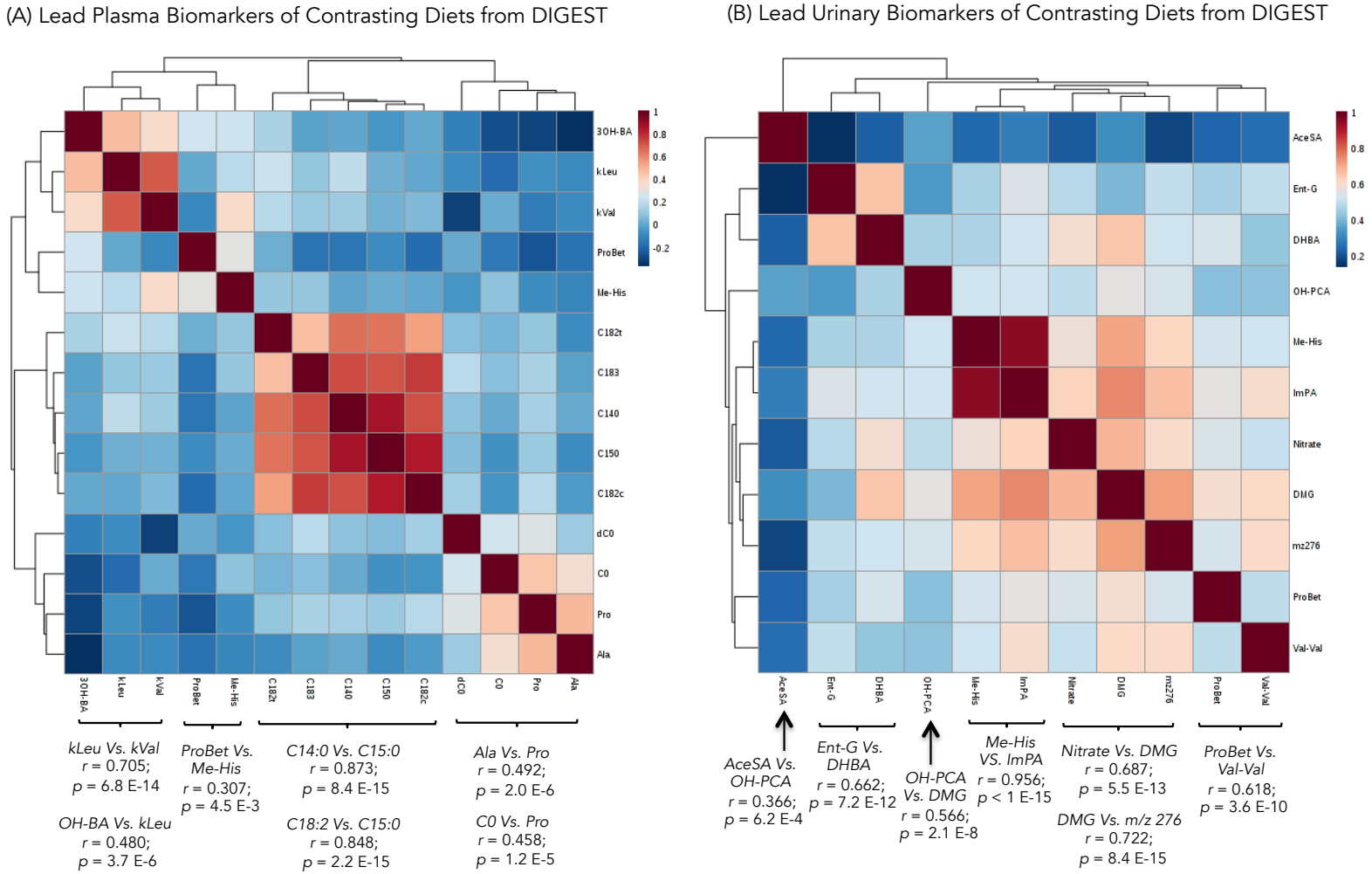

Figure S14. 2D heat maps and correlation matrices for top-ranked (A) plasma and (B) urinary metabolites associated with contrasting diets from food provisions when using a Pearson correlation analysis on *glog*-transformed data. Distinctive clusters of metabolite classes suggest common dietary sources and/or biochemical pathways for their regulation, such as circulating ketone bodies (kLeu, kVal, 3-OH-BA), fatty acids (C14:0, C15:0, C18:2, C18:3) and amino acids/carnitines (C0, Pro, Ala) in plasma, as well as plant-derived biotransformed phenols (Ent-G, DHBA) and imidazole metabolites (Me-His, ImPA) in urine. In many cases, urinary metabolites reflective of recent dietary patterns were broadly co-linear with other compounds (*e.g.,* OH-PCA, Me-His, ProBet and unknown ion, *m/z* 276) or had modest correlations (*e.g.,* AceSA) to other compounds overall.